Antarctic Research, Vol. 4, No. 2, 42～61, December 1993

PSEUDOINVERSE DETERMINATION OF THE CIRCULATION IN PRYDZ BAY AND ITS ADJACENT OPEN OCEAN, ANTARCTICA

Liang Xiangsan[1](梁湘三), Su Jilan[1](苏纪兰) and Dong Zhaoqian[2](董兆乾)

[1] *Second Institute of Oceanography, SOA, Hangzhou 310012, China*

[2] *Polar Research Institute of China, Shanghai 200129, China*

Abstract An inverse model is used to infer the circulation in Prydz Bay and its adjacent open ocean using hydrographic data obtained by the cruise of the 7th Chinese National Antarctic Research Expedition (CHINARE-7), 1990/91. Barotropic components are found to be strong in the study area, esp. at the Antarctic Divergence, and from a whole view, the velocity is rather small. In the open ocean, the flow is quasizonal, but outside the bay it shows a tendency of pressing onto the shelf from surface to bottom, and a feature of intensification just east of Fram Bank. We suggest here be the most important place to detect the possibility of the Antarctic Bottom Water formation. The meridional profiles of the distribution indicate a strong (relative to the ambient) core and a slope-trapped part into the bargain. In the southeastern part of the bay, there seems to exist a strong coastal current flowing westward. The computed upwelling centers are mainly situated in the west of the study region, as agrees quite well with the early hydrographic observations and the areas of high krill biomass.

Key words Prydz Bay, pseudoinverse, barotropicity

Introduction

The present study area lies south of 62°S and between 68° and 93°E, including Prydz Bay and its adjacent region (Fig. 1). Here the topography is typical of Antarctic Oceans, with a steep slope immediately off the continental break and a depression on the shelf, which is characterized by a basin. The greatest depth within Prydz Bay (1085m) is adjacent to the Amery Ice Shelf. To the northeast and northwest are two banks, less than 200m at the shallowest points.

In the Antarctic oceans, air-ice-sea interaction is significant. Over the study region, in the north the Westerlies prevail all year round, while in the south the Polar Easterlies is dominated. Between the East and West Wind Drifts there exists a divergence zone, which is usually referred to as Antarctic Divergence. In the austral winter, all of the sea surface is ice-covered. During late spring and early summer, the ice cover begins to break and melt

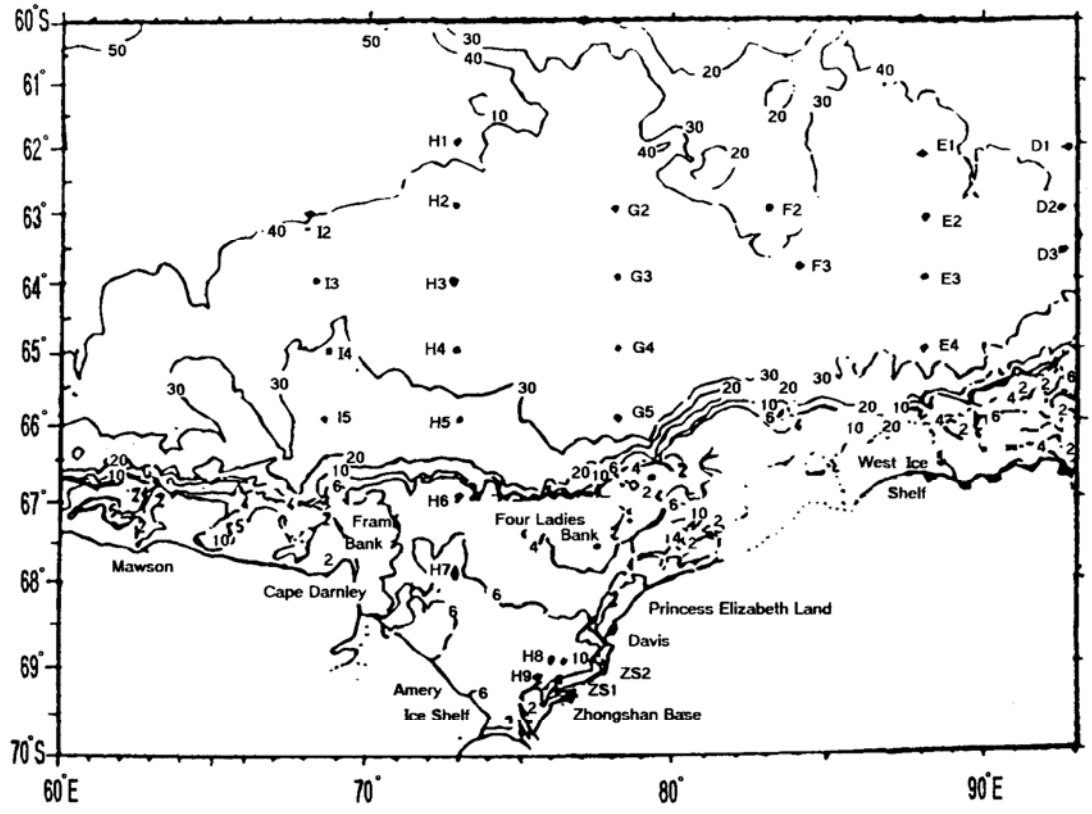

Fig. 1. Geographical and topographical features in the study area.
The isobaths are marked in units of 100m (from Dong *et al.*, 1984).

gradually from north to south. In midsummer, the fast ice breaks, too, but patches of floes still cover most of the shelf regions. Dong *et al.* (1984) found that at this time the ice conditions in Prydz Bay varied rapidly.

As for the characteristics of the circulation in Prydz Bay and its adjacent deep ocean, the predecessors have made some descriptions using the scarce observations. In the open ocean outside the bay, the chart of dynamic height of Zverev (1963) showed here existed a large-scale cyclonic gyre, which centered at the Divergence zone. Smith *et al.* (1984) pointed out, after processing the cruise data of the First International BIOMASS Experiment (FIBEX) Voyage *MV Nella Dan*, January-March 1981, that there appeared another gyre with similar features. By the adjusted steric height relative to 300 dbar they calculated, the flow seemed to be very weak. In the shelf region, by computing the geostrophic flow using Defant's method to define the no-motion level, Grigor'yev (1967) found the circulation in Prydz Bay is characterized by a cyclonic gyre centered on the deep waters, which is stronger in the southeast. At the same time, Yeskin (1967) noted there was little water exchange between Prydz Bay and Davis Sea to its east beneath the West Ice

Shelf. In 1984, the first time Smith *et al.* described in detail the water masses and circulation in the Prydz Bay region. While confirming the existence of the clockwise gyre, they found a cold current flowing into the southern part of the bay from the region of the West Ice Shelf, which tended to strengthen in the past several years. Recently, there has been a trend of interest in the study of the vertical convection in the bay. Shi (1991) concludes that there must exist an independent special vertical circulation system to balance the heat and salt budget during ice congelating and melting, precipitating and solar irradiation, etc.

Although the former oceanographers have done a lot about the circulation in Prydz Bay region, all of them describe only the geostrophic flow relative to some presummed levels of no motion. In the Antarctic oceans, however, such flow patterns cannot tell much due to the strong barotropicity (Gordon, 1983). Hence, here we shall use an inverse model to process the observed data, and obtain the corresponding barotropic components. In the present paper, section 2 presents the data set and its preliminary treatment, section 3 describes briefly the model's formation, and section 4 gives the technique to select an optimum solution among the candidate pseudoinverse vectors. Secton 5 gives the results and discussions. We divide this section into two parts: One for the horizontal pattern, while the other for the vertical circulation. In the last, a brief summary is presented.

The Data Set and Preliminary Data Treatment

The data used for the inverse calculation is the one obtained by the cruise of the 7th Chinese National Antarctic Research Expedition (CHINARE) from December 1990 to February 1991. Six sections (D to I), together with Sta. s No. ZS1 and ZS2, are deployed, and in total there were 28 CTD profiles available in the study area. The stations shown in Fig. 1 are arranged generally in a regular grid, with one degree spacing in latitude and five degree in longitude. In Amery Basin, the four stations, Sta. s H8, H9, ZS1 and ZS2 are treated as a single point. The summer water mass structure in Prydz Bay and its adjacent open ocean is characterized by the distinct modal properties of Antarctic Summer Surface Water (AASSW), Circumpolar Deep Water (CDW), Antarctic Bottom Water (AABW), Antarctic Winter Water (WW), Continental Shelf Water (SW) and Ice Shelf Water (ISW) (c. f. Fig. 1. 10 of Dong *et al.*, 1984). As shown in Fig. 6, these features have been reflected in the cruise data, but perhaps due to internal waves, every profile exhibits some fine structures. For this reason, they are smoothed by a 20 meter running average, and subsampled in the vertical to obtain potential temperature, salinity and density at 29 standard depths specified by the model grid.

Model Description

Because we don't get the full-depth data, the integration method of Wunsch (1977), accurate as one tends to think, cannot be exploited here. Instead, the inverse model presented below uses advection-diffusion equations for the temperature and salinity (Tziperman and Hecht, 1988) to calculate the absolute geostrophic velocity field:

$$
\begin{cases}
fu = -(1/\rho_0)p_y & (1)\\
fv = (1/\rho_0)p_x & (2)\\
p_z = -g\rho & (3)\\
u_x + v_y + w_z = 0 & (4)\\
uT_x + vT_y + wT_z = [K_v(z)T_z]_z + K_H(z)\nabla_H^2 T & (5)\\
uS_x + vS_y + wS_z = [K_v(z)S_z]_z + K_H(z)\nabla_H^2 S & (6)
\end{cases}
$$

where u,v,w and velocity components in x,y,z directions, respectively, and ρ is density, P is pressure, T is temperature, and S is salinity. In Eq. s(5) and (6), the mixing of salt and heat are parameterized with horizontal and vertical eddy mixing coefficients (K_H and K_V, respectively) which are possibly functions of depth. Tziperman and Hecht (1988) have argued that it is reasonable to use them to replace the cross- and along-isopycnal mixing coefficients without introducing large errors. And they also pointed out, through experiments, these coefficients can only be partly resolved, and adding the horizontal mixing cannot improve the results significantly, so here it is decided to include only the vertical one in the model because one tends to trust vertical derivatives of the high vertical resolution of CTD data more than horizontal ones taken from the sparsely spacing station data.

The simple expressions of the mixing processes in Eq. s (5) and (6) is somewhat unsuitable in the Prydz Bay due to the patches of ice floes. The unreasonably large velocity at the point near the Zhongshan Station presented later may have something to do with this distorted description of the thermohaline processes.

The geostrophic assumption in Eq. s (1) and (2) doesn't seem to be valid in the shelf region, either. However, the slow processes it bears are of great reference value. With this approximation, the velocity is horizontally nondivergent, and the principle of mass conservation demands the invariance of the vertical velocity with respect to depth. This may lead to the inconsistence of the surface vorticity input by the wind with the bottom boundary condition. But because W is very small (an order of 10^{-4}cm/s), this geostrophic assumption is expected to be satisfactory beyond the surface and bottom Ekman layers.

From the geostrophic and hydrostatic equations, the thermal wind equations are obtained:

$$\begin{cases} fu_z = \dfrac{g}{\rho_0}\rho_y & (7) \\ fv_z = -\dfrac{g}{\rho_0}\rho_x & (8) \end{cases}$$

Integrating these equations in z, from a reference level, $z=z(x,y)$, the vertical structure of the horizontal circulation is found in terms of the known density field. The full velocity field can be written as:

$$\begin{cases} u(x,y,z) = u_0(x,y) + \displaystyle\int_{z_0}^{z} \frac{g}{\rho_0 f_0}\rho_y dz & (9) \\ v(x,y,z) = v_0(x,y) + \displaystyle\int_{z_0}^{z} \frac{g}{\rho_0 f_0}\rho_x dz & (10) \\ w(x,y,z) = w_0(x,y) & (11) \end{cases}$$

where u_0, v_0 and w_0 are the unknown velocities at the refernce level.

Substituting the velocity field (9), (10) and (11) into (5) and (6), after neglecting the horizontal diffusion, gives:

$$u_0(x,y)\cdot T_x(x,y,z) + v_0(x,y)\cdot T_y(x,y,z) + w_0(x,y)\cdot T_z(x,y,z) - [K_v(z)\cdot T_z]_z = \Gamma_T(x,y,z) \quad (12)$$

$$u_0(x,y)\cdot S_x(x,y,z) + v_0(x,y)\cdot S_y(x,y,z) + w_0(x,y)\cdot S_z(x,y,z) - [K_v(z)\cdot S_z]_z = \Gamma_S(x,y,z) \quad (13)$$

where Γ_T and Γ_S represent the advection of T and S by the known relative velocities in (9), (10) and (11).

Following Hogg (1987), the mixing coefficients are expanded in Chebyshev polynomials

$$K_v(z) = \sum_{n=0}^{N_v} C_{v,n} T_n[f(z)] \quad (14)$$

where f(z) is a dimensionless function of z to be determined. Since

$$[K_v(z)\cdot S_z]_z = \sum_{n=0}^{N_v}\left[C_{v,n}T_n S_{zz} + C_{v,n}\frac{dT_n}{dz} S_z\right] \quad (15)$$

we should choose $f(z) \in (-1,1)$ to ensure the nonsingularity of T_n and dT_n/dz. Here $f(z)=z/D$ is chosen, and D is greater than the maximum data-available depth for all

stations.

Now, evaluating the derivatives in Eq. s (12) and (13), as well as the geostrophic velocities relative to the reference level, we obtain linear equations for the unknown reference velocities and mixing coefficients. These equations can be formed at any level where data is available. But since more levels do not mean better resolution, only six are taken into account. Thus formed equation set

$$\mathbf{A}\,\mathbf{X} = \Gamma \tag{16}$$

has 290 equations, with 85 unknowns to determined (if retaining only the first 10 terms in (14)). Eq. s (16), together with six inequality constraints

$$K_v(z) \geqslant 0 \tag{17}$$

constitute a linear inverse problem (c. f. Wunsch, 1977). It should be noticed that this problem is rank-deficient and is always underdetermined though in (16) the number of equations exceeds greatly that of unkowns. We solve it by means of a method termed Singular Value Decomposition (SVD), which can be found in Lawson and Hanson (1974).

Selection of an Optimum Solution

A series of solutions are obtained when solving (16) subject to (17). Selection of an optimum one among the candidates is determined by matrix analyses and physical constraints (minimizing the errors as well as the bottom brotropic energy).

The first and key problem one must solve is how to find an appropriate pseudorank of **A**. Tziperman and Hecht (1988) selected it so that the horizontal velocities were always resolved, the mixing coefficients partly resolved and the vertical velocities unresolved. Since we have no idea in advance if these unknowns are resolved or unresolved, we'll select the pseudorank in another way.

Such pseudorank is related to the preliminary treatment of **A**, which in the present paper means its column scaling:

$$\tilde{\mathbf{A}} = \mathbf{A}\,\mathbf{D}$$

If **D** is $n \times n$ nonsingular, this transformation doesn't change the problem itself mathematically. However, unless **D** is orthogonal, the condition number of $\tilde{\mathbf{A}}$ will generally be different from that of **A**. Thus one may decide to choose **D** with the objective of making

COND($\tilde{\mathbf{A}}$) small. Here the method of Lawson and Hanson (1974) is effective:

$$D_{jj}=\begin{cases} \| a_j \|^{-1} & \text{if } \| a_j \| \neq 0 \\ 1 & \text{if } \| a_j \| = 0 \end{cases} \tag{18}$$

where a_j denotes the jth column vector of **A**. It has been proved by Van der Sluis (1969) that with **D** defined by Eq. (18), using euclidean column norms, COND(**AD**) doesn't exceed the minimal condition number obtained by column scaling by more than a factor of $n^{1/2}$.

We get the singular values of the scaled matrix arranged in an order from the maximum to the minimum, and shown in Fig. 2. Compared with the results without scaling (Figure not shown), the singularity is reduced greatly. By Fig. 2, the pseudorank should be selected

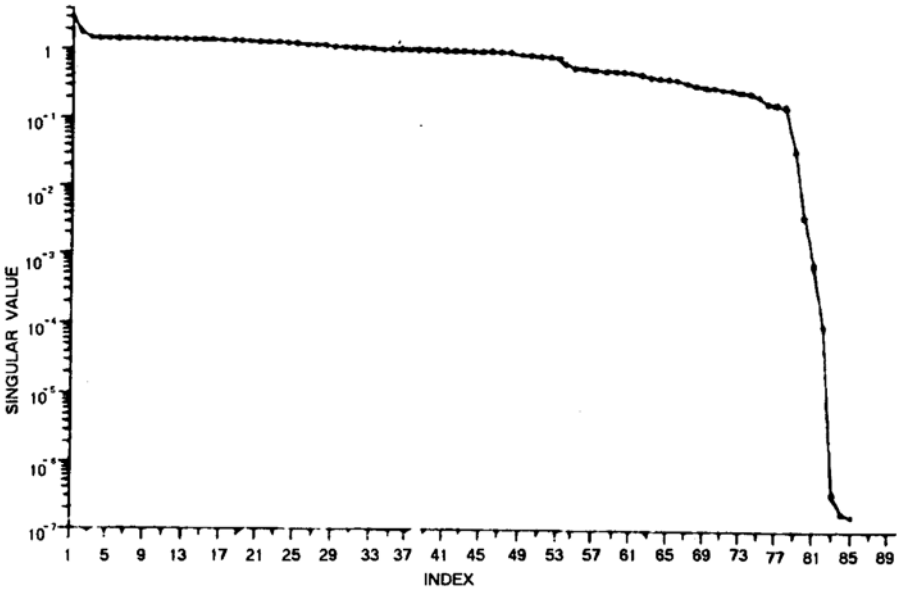

Fig. 2. Singular value versus index.

smaller than 79.

There must be a compromise between error and solution norm (hence the bottom barotropic energy) minimization. The diagram of residual norm $\| \mathbf{r} \|$ versus solution norm $\| \mathbf{X} \|$ (Fig. 3) suggests an optimum selection of Rank(**A**)=77, subject to (17). It should be noticed that at this time the null space is relatively small, and hence the solution obtained might be unphysically large if the pseudorank is chosen by minimizing the euclidean norm of the residual vector. Fortunately, Fig. 3 shows most of the candidate solution points fall within a small range of the solution space. Hence the matrix behaves well, and it isn't easy for such phenomenon to take place.

The above-mentioned pseudorank is only an optimum selection, and in this problem,

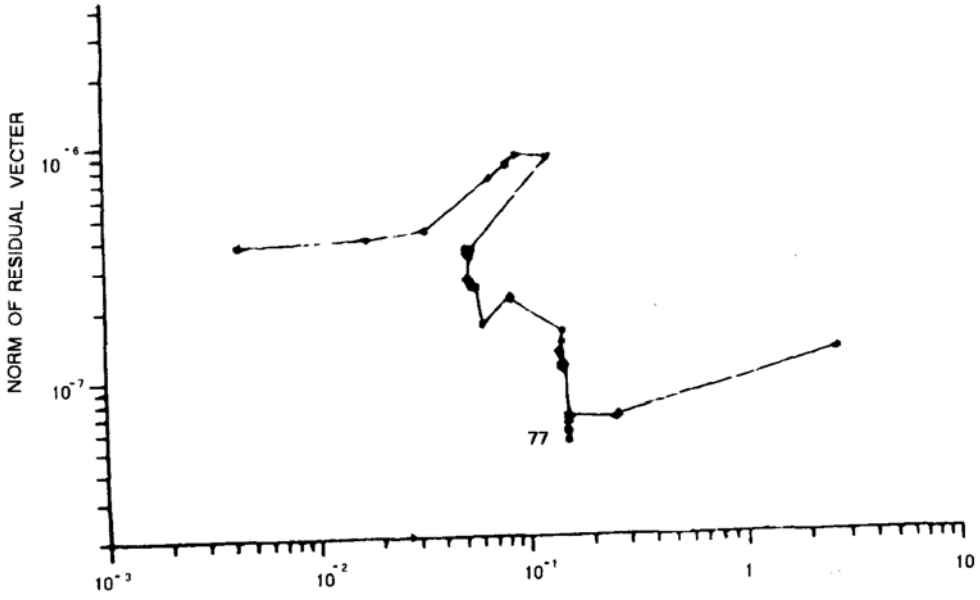

Fig. 3. Residual norm versus solution norm.

there're still a number of alternatives one cannot find sufficient evidences to abandon. We have noted, among these candidates, the horizontal velocities vary rarely, while $K_v(z)$ varies a lot, as agreed with Tziperman and Hecht (1988). What needs elucidating is the vertical components, w_0, parts of which change little, too. Consequently, they can be also partly resolved. By the cruise data, the norm of the error matrix of **A**, $\| \mathbf{E} \|$, is 6.4×10^{-3}, and the deviation of $\| \Gamma \|$, $\| d\Gamma \|$, is about 1.8×10^{-8}. As established by Lawson and Hanson (1974), $\| d\Gamma \| / \lambda_i$ (λ_i, the singular values) gives the standard deviation of P_i, the solution after orthogonal transformation. The pseudo solution vector with Rank(**A**) = 77 indicates there're 15 P_i s smaller than their corresponding standard deviations. Thus even if all of the 10 components of the mixing coefficient were well resolved (In fact they can be partly resolved, c. f. Tziperman and Hecht (1988) and Needler and Heath (1975).), there are still ten w_0s credible in some way.

This mathematical phenomena, as it were, might have something to do with the significant vertical convection in the study region (Shi, 1991). Hence in (5) and (6), the importance of wT_z should be taken seriously as well as the horizontal advective terms. As a matter of fact, even if wT_z/uT_x is an order of 1/7, as estimated by Tziperman and Hecht (1988), it won't always fall into the relative error range of the solution. According to Lawson and Hanson (1974):

$$\frac{\| d\mathbf{X} \|}{\| \mathbf{X} \|} \leqslant \hat{\kappa}\alpha + \hat{\kappa}\gamma\beta + \hat{\kappa}\kappa\rho\alpha + \kappa\alpha \qquad (19)$$

where

$$\alpha = \frac{\| \mathbf{E} \|}{\| \mathbf{A} \|}, \qquad \beta = \frac{\| d\Gamma \|}{\| \Gamma \|}, \qquad \gamma = \frac{\| \Gamma \|}{\| \mathbf{A} \| \cdot \| \mathbf{X} \|},$$

$$\rho = \frac{\| \mathbf{r} \|}{\| \mathbf{A} \| \cdot \| \mathbf{X} \|}, \qquad \kappa = \| \mathbf{A} \| \cdot \| \mathbf{A}^{+} \|, \qquad \overset{\wedge}{\kappa} = \frac{\kappa}{1-\kappa\alpha}$$

and $\mathbf{A}^{+}$ is the pseudoinverse of $\mathbf{A}$. By the computational results of this problem

$$\frac{\| d\mathbf{X} \|}{\| \mathbf{X} \|} \leqslant 0.04$$

and this is only the upper limit. So what we obtain about the distribution of the vertical velocities is credible in a sense, or at least the positive and negative signs are credible. This sign distribution enable us to find the upwelling area in the study region (more about it later).

Sometimes the inverse model exploited in this paper can infer mixing coefficients as well as the velocity field. Here we are not to make discussion about it, and only give our results for reference:

$$K_v(z) = \sum_{n=1}^{10} C_{v,n} T_{n-1}(z/1200)$$

where $T_n (n = 1, 2, 3, \ldots)$ is Chebyshev polynimals, and $C_{v,n}$ can be written as a vector form:

$$C_v = (1.09\times10^{-6},\ -8.94\times10^{-9},\ 3.76\times10^{-8},\ 5.70\times10^{-9},\ -1.18\times10^{-7},$$
$$-6.67\times10^{-9},\ 5.08\times10^{-8},\ 8.18\times10^{-9},\ -1.98\times10^{-8},\ -9.73\times10^{-9})^{T}$$

Analysis of the Results

(1). Features of horizontal circulation.

By experiments, varying the reference level exerts few influences on the final results. Taking the deepest data-available level as reference, we get the surface flow pattern depicted in Fig. 4, from which one will find that the flow is generally weak in our study area, and the maximum surface velocity among all the stations can only reach 6 cm/s or so, except the one near the Zhongshan Station. It should be pointed out that the above-mentioned geostropic approximation might not be appropriate in shelf regions, so the computed velocity at this point can only be used for reference. Experiment has been done without this solitary

station, and it reveals almost the same velocity field outside the bay. Consequently, the velocity in the open ocean is rather small. As a matter of fact, at such a high latitude, the West Wind Drift becomes very weak, and Smith *et al.* (1984) also reported that here the geostrophic flow is an order of several centimeters per second. In a word, our results are consistent with the early studies.

Fig. 5 is the hydrographic diagram at the surface level, and Fig. 6 shows the temperature and salinity distribution on Section H. From them one cannot find any inditation of strong current, either.

Another feature of interest about the circulation in the study area is its strong barotropicity, and the barotropic components are comparable to the baroclinic ones, as can be seen in Fig. s 7 to 10. Fig. 9a shows the distribution of absolute velocity on Section G, where the isolines reach the bottom without closing, in sharp contrast to its geostrophic counterparts relative to some assumed level of no motion (Fig. 9b). There is, of course, some kind of uncertainties using pseudoinverse-seeking method to obtain the velocities. However, we select our solution vector by minimizing its euclidean norm hence the bottom barotropic energy (Wunsch, 1977) as well as the residual norm (hence the measurment and turbulent errors), and, as stated above, though the null space is small, on the diagram of $\| \mathbf{r} \|$ versus $\| \mathbf{X} \|$ the candidate solution points almost amass in a small range of the solution space, therefore even if our results were doubtful, what one can only say is that they might have been underestimated, or, in other words, perhaps the barotropicity of the real flow field is even stronger. In fact, from a global view, the Antarctic oceans is the region of ventilation, and as pointed out by Gordon (1983), baroclinicity is very weak within the nearly homogeneous water column south of the Antarctic Circumpolar Current (ACC), and the likely dominance of barotropic components south of the ACC means that geostrophic flow relative to some zero speed reference level does a poor job of defining the circulation.

Before going further into the delineations, it is useful to organise our discussions in two ways. In the following, we'll present firstly the meridional section profiles and then the horizontal flow patterns.

a. Meridional profile

(a) Section H (73°E)

Fig. 7 is the vertical distribution diagram of the zonal velocity on Section H, from which it is easy to see that water flows eastward north of 67°30′S, and, in particular, between 64° S and 65°S exists a relatively strong current core.

The maximum surface velocity reaches to 3. 5 cm/s. Near 65°30′ and 66°S, the velocity varies rapidly in meridional direction, but south further, its gradient becomes small, and a second strong region appears near 67°S. Checking it against Fig. 1, one will find this second strong area is right at the continental slope. As a result, a part of flow has been

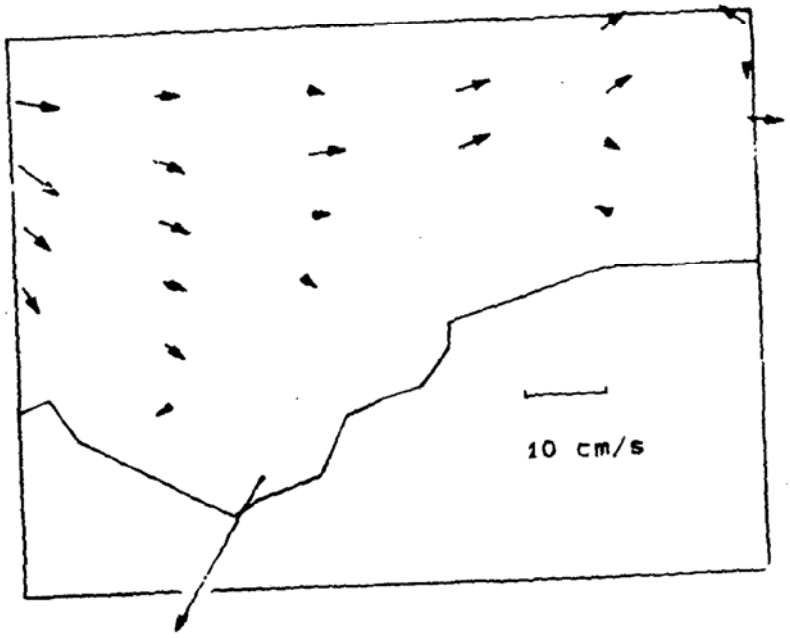

Fig. 4. Absolute velocity field at sea surface.

trapped by the shelfbreak zone. Around 67°30′S, the flow reverses its direction. This transient position between the East and West Wind Drifts is consistent with Shi (1991).

The above-obtained velocity distribution can also be illustrated in the meridional hydrographic profiles (Fig. s 6a,b). In Fig. 6a, by the definition of Smith *et al.* (1984), the layer between 0 and 50m is occupied by the Antarctic Summer Surface Water (AASSW). Beneath 100m or so, north of 66°30′S is the Circumpolar Deep Water (CDW). And below the highly variable AASSW and above the CDW mass lies a temperature mimimum layer that is believed to be the remnant of winter time convection and is termed Antarctic Winter Water (WW). Over the shelf, there exists an even colder shelf water (SW). Between depth 80 and 120m, a solitary mass separates the WW from the SW at 65° S, marking the sharp front noted by Smith *et al.* (1984). Such a temperature structure, in addition to the somewhat crowded isohalines here, suggest a relatively strong current immediately north of this latitude. As regard to the interface of the west and east wind drifts, it is reflected to some extent in Fig. 6b, too. In this figure, near 67°S the surface salinity is higher than the ambient, and hence the isohaline here arches upward, indicating the slope-trapping of the west wind drift north of 67°S, as well as the reversal of the flow direction south of this latitude. Besides, this diagram indicates here exists of some kind of upwelling phenomenon. We'll present more about them later.

(b) Section I (68°20′E)

As shown in Fig. 8, the structure of the zonal flow distribution on Section I can be summarized as: Eastward; Strong to the north and weak to the south. Since the

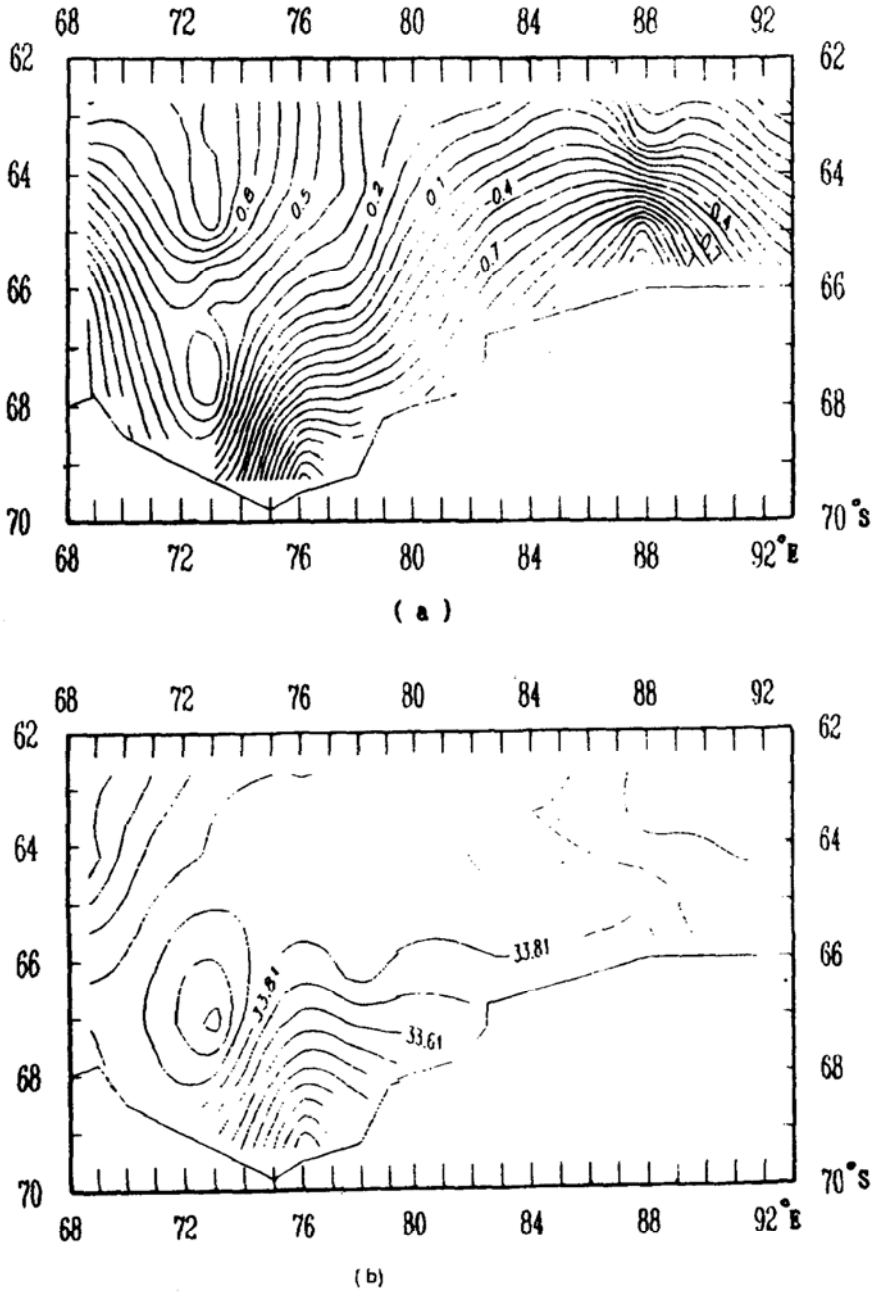

Fig. 5. Surface temperature (a) and salinity (b) distribution.

hydrographic stations don't occupy the region south of 66°S, the East Wind Drift finds no way in this figure. In the north, most of the flow concentrates in the upper layer, while in the south, barotropic component dominates and this diagram exhibits an almost homogeneous vertical structure. On this section, the surface eastward velocity maximizes at 63°S, with a value of 5.1 cm/s.

(c) Section G (78°E)

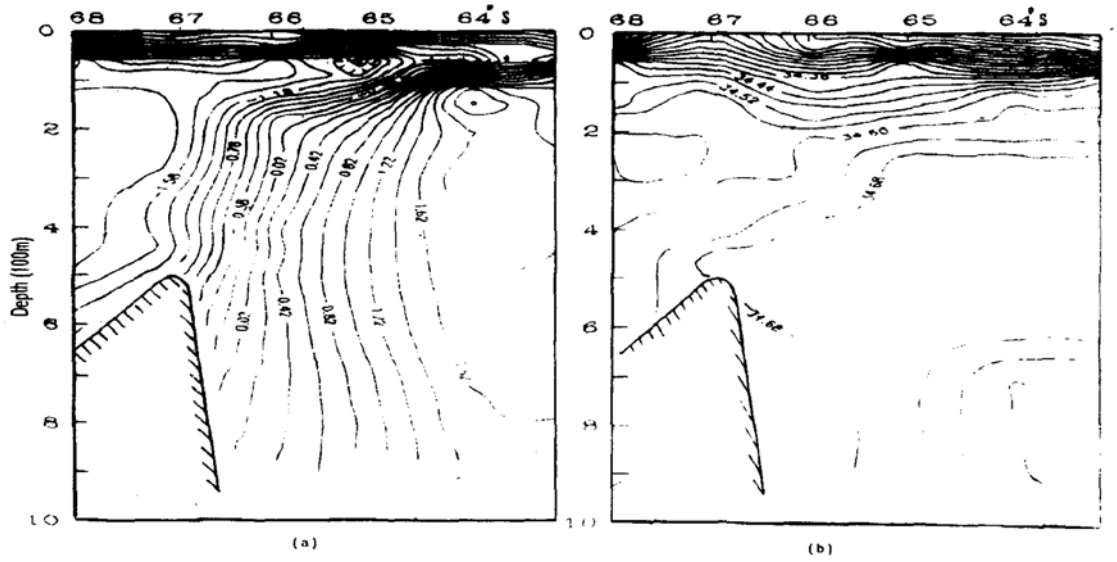

Fig. 6. Temperature (a) and salinity (b) distribution on Section H.

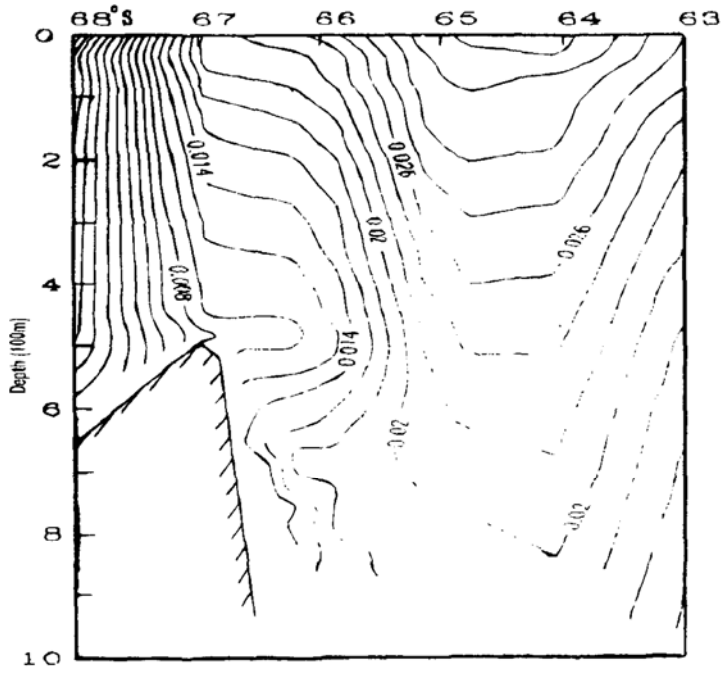

Fig. 7. Zonal velocity distribution on Section H.

A distinct feature of the velocity distribution on Section G is illustrated in Fig. 9a that around 64°S forms a narrow core of strong current (relative to the ambient), which goes

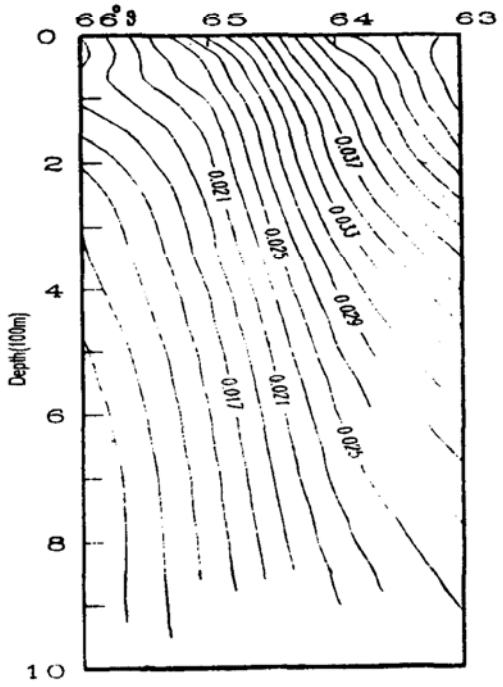

Fig. 8. Zonal velocity distribution on Section I (unit: m/s).

down to the deepest data-available level. In this region the current is particularily strong at upper to 100m level, and its maximum surface velocity can reach to 4. 2 cm/s. In fact, here is right at the position where WW and SW intersect (Figure omitted). South of 64. 5°S, the barotropic flow dominates, and the meridional distribution south of 65°S tends to be uniform.

(d) Section E (88°E)

In Fig. 10, north of 64°30′S the flow is relatively strong, and at 65°S there's some indications of the East Wind Drift (c. f. Fig. 4). At about 64°S, a strong shear band appears, marking the trasient zone from the West to the East Wind Drifts.

b. Horizontal Distribution

(a) Open Ocean Circulation

Early studies (e. g. , Smith *et al.* , 1984) demonstrated that in the open ocean adjacent to the Prydz Bay there exist two large scale cyclonic gyres, centering at the Antarctic Divergence. Our results (as shown in Fig. 4) reveal some indications of them morth of West Ice Shelf and Cape Darnley, but the velocities are so small that they cannot elucidate too much. On Section D, it seems that there exists another relatively small scale anticyclonic gyre.

Because of the sparse measurements and hence the large spans between stations, some relatively small scale structures, such as mesoscale eddies, cannot be resolved, and we'll keep our eyes mainly on the large-scale characteristics.

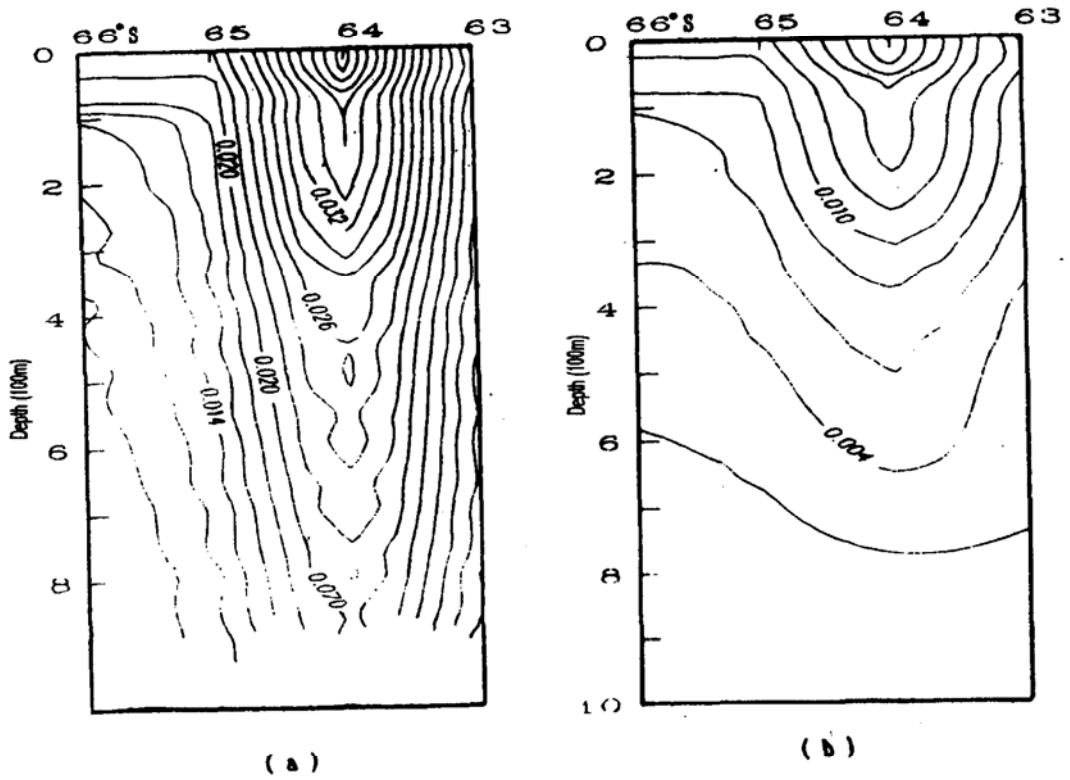

Fig. 9. Distribution of absolute zonal velocity (a) and its geostrophic counterpart relative to 850m level (b) on Section G.

From the flow patterns at surface (Fig. 4), 100m and 700m levels (Fig. s not shown), it is easy to see that the current rarely changes its direction from surface to bottom, and from a whole view in the computational domain, it exhibits an anticyclonic pattern. After entering the study area from north of Cape Darnley, the current in the southern part flows round the Fram Bank, approaching the slope and showing some tendency of intruding onto the shelf and then looping back, making its original way eastward. Around Station E1, the flow is somewhat divergent because of the shallow Gribb Bank.

This interesting feature, though none have been reported before, does find its way in some hydrographic diagrams of previous studies. It was noted by Smith *et al.* (1984) that the warm, deep CDW tended to press to the shelf near West Ice Shelf and to the east of Fram Bank (c. f. Fig. 9 of their paper). Our temperature distribution at surface (Fig. 5) and 150m levels confirm it, too. As a matter of fact, such a departure from its original path has its dynamical foundations. Su and Pan (1987) have made some discussions on it, and have found a lot of evidences, including the observational and computational ones, in the Kuroshio region north of Taiwan in the East China Sea. They pointed out, in that area, topographical beta effect makes the signals from the north diffused southward, and the island-edge boundary layer fast to Taiwan will trap them, and hence provide a dynamical

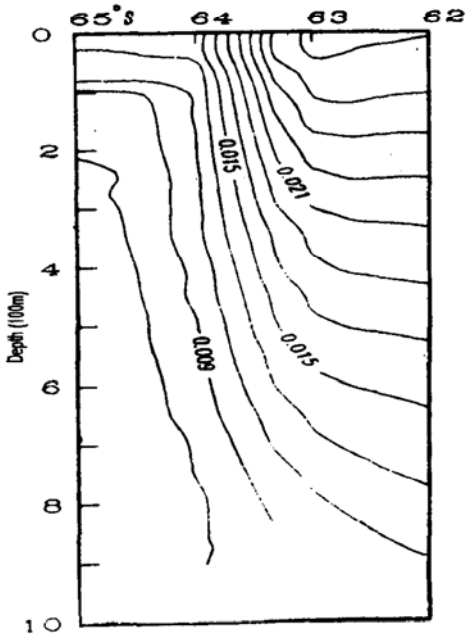

Fig. 10. Zonal velocity distribution on Section E.

mechanism for the Kuroshio's westward intrusion, making it intensified towards the island. In the sounthern hemisphere, of course, things are different. In the present study area, the contribution of the topography to the vorticity budget appears as

$$-\frac{f}{h}\frac{\partial h}{\partial y}v,$$

where $f<0$. The topographic beta effect $-\frac{f}{h}\frac{\partial h}{\partial y}>0$, together with the planetary beta effect, will lead to the westward propogating of the signals from east. Though there doesn't exist a solid boundary north of Cape Darnley, the Fram Bank offers some possibilities for such kind of shelfward 'pressing'. Therefore, it is reasonable to anticipate the CDW's intruding onto the shelf if there were a strong current flowing eastward rightly north of the slope.

(b) Shelf circulation

Since the stations are very scarce over the shelf, and since the above- mentioned geostrophic assumption may not be appropriate due to the comparable large Ekman thickness, what we have calculated in this shallow region is presented for reference only.

The previous studies, such as Grigor'yev (1967) and Smith *et al.* (1984), demonstrated that the circulation of the Prydz Bay is characterized by a cyclonic gyre, in addition to a westward coastal current along the West Ice Shelf and Mawson Coast. Fig. 4 exhibits some indications of this pattern, but one cannot draw conclusions from them

because of the trifling velocities.

The significant point lies outside the Zhongshan Station, where the surface absloute velocity reaches as large as 22 cm/s, and its relative geostrophic counterpart reaches to 10 cm/s, too. It is still unclear why it is so strong. Maybe because of the harsh ice conditions and hence the significant sea-ice-air interactions at this particular position, we must add some corresponding terms to the right-hand sides of Eq. s (5) and (6); or perhaps here the data its own is doubtful. But as reported by Grigor'yev (1967), it is true that in the Prydz Bay the velocity is unevenly distributed, and southeast of the main gyre it is expected to come to as large as 9. 2 cm/s.

Now, where does this cold current come from? Smith *et al.* (1984) assumed it originated in the surface water off the shelf, and some of the water might have originated from the shelf between the Shackleton and West Ice Shelves. They found that icebergs off the Princess Elizabeth Land always moved southwest, while those calved from the Amery Ice Shelf normally followed the western periphery of the Prydz Bay towards Cape Darnley. These evidences confirm the existence of this littoral current. Further more, these years the icebergs off the Davis Station have been increasing rapidly, suggesting the strengthening of this cold current after the Chelyuskintsy Ice Tongue broke off. With these evidences, our result at this point seems reasonable in some way. Besides, from a dynamical view, once this current pernetrates into the bay, the unique bathymetry hence topographical beta effect, will make it intensified towards the eastern boundary. As a result, so long as there exists a current in the bay, it is sure to be most significant in the east. For this reason, at least our result can tell something qualitively.

2. Features of vertical circulation

As for the features of vertical circulation in the Prydz Bay, Shi (1991) has presented a relatively detailed description of them. As stated before, it is due to the existence of the significant convection system, that the vertical velocities can be partly resolved in the pseudoinverse-seeking process. To verify this the computed upwelling centers are depicted, as shown in Fig. 11. The two upwelling centers in the east are insignificant, and we'll keep our eyes mainly on the two in the west. The upwelling center over the shelf (67°S, 73°E) has been reported by Shi (1991). Immediately north of it appears downwelling phenomenon. North of 65°S is another wide upwelling area, which is closely related to the above-mentioned possibility intruding tendency of the CDW. Why anticyclonic meandering will sometime and somewhere abnormally induce upwelling has been interpreted in detail by Liang and Su*. These convection processes take the high-temperature and high-salinity

* Lian Xiangsan and Su Jilan: A two-layer model for the circulation in the East China Sea. *Acta Oceanol. Sinica* (in press).

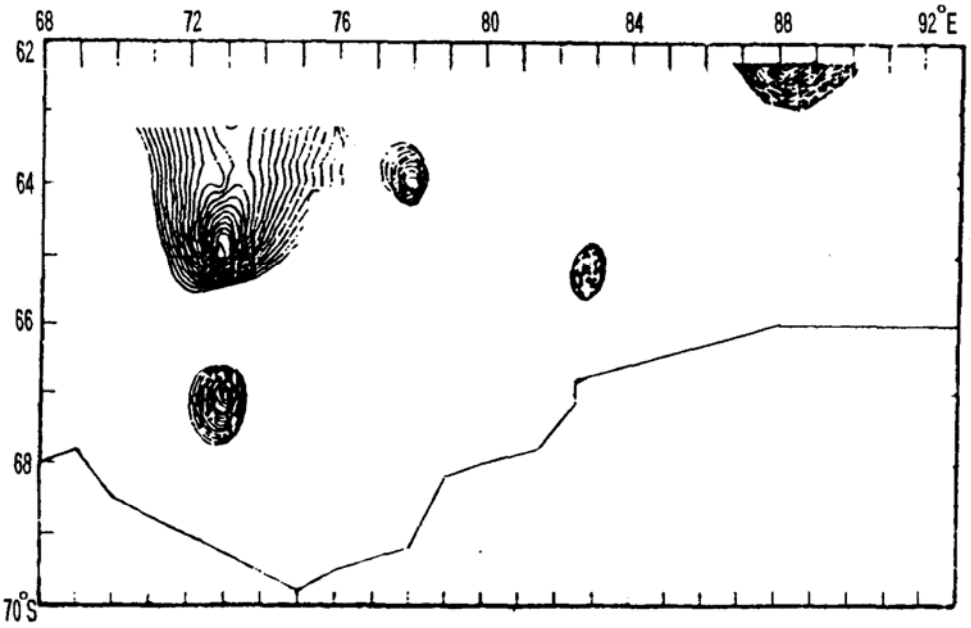

Fig. 11. The computed upwelling centres.

water upward, leading to the apparently early appearance of ice-free open waters in the western part of the bay (Smith *et al.*, 1984). Mellor (1960) also reported polynyas between Cape Darnley and Mawson Station during spring while the sea is still covered elsewhere. Thus it can be seen that the distribution of the vertical velocities obtained in this paper is in a sense credible.

Hydrographic diagrams (e. g., Fig. 6) provide evidences for the apearance of the two upwelling centers, too. In the salinity distrbution diagram at 150m level (Fig. omitted), the two high salinity areas in the west correspond the two centers in Fig. 11. Between them is a lower salinity region. The surface temperature and salinity distributions show a high-temperature and high-salinity center at 67°S, 73°E, whose origin can be traced from the upwelling of the relatively warm and saline CDW.

It is interesting to find, while comparing Fig. 11 with the krill distribution diagram (Marr, 1962), that the two areas happen to be these places with a high biomass. From the present results, maybe this distribution has something to do with the upwelling events.

Summary and Conclusion

Since the late seventies of this century, there has been an upsurge of interest in the determination of absolute velocity fields from measurements of conservative quantities such as temperature and salinity. In the present paper, the inverse model of Tziperman and Hecht (1988) is used to treat the cruise data of the 7th CHINARE, and infer the flow

pattern in the Prydz Bay and its adjacent open ocean.

In the study area, esp. the Antarctic Divergence, strong barotropicity is found to characterize the circulation, and the meridional section profiles of zonal velocity show that the isolines almost go straight down to the deepest data-available level, without any indication of closing. This suggests the geostrophic flow relative to some no-motion reference cannot tell much here. Besides, by our calculation, except the point near the Zhongshan Station, the horizontal flow field is very weak, with a maximum surface velocity less than 6 cm/s.

In the open ocean outside the bay, the flow is quasizonal, with a relative strong core on the meridional section. This current core, as it were, appears at about 63°S on Sections I and E, and at 64°S on Section G. On Section H it moves southward, at about 64°30′S. There're also some flows trapped on the slope. Horizontally, there seems to exist a strong coastal current in the east part of the bay, and those gyral structures noted by the former oceanographers have been reflected in some way, but what features most is the tendency of the eastward current's pressing on the shelf at all levels, from surface to bottom. We think it is due to the topographical and planetary beta effects. If some kind of intrusions do exist, the two mechanisms will make them intensified towards the Fram Bank. Since the CDW's rising and extending onto the shelf is a key element in AABW formation (Gill, 1973), we should pay particular attention on the region immediately east of the Fram Bank if attempts are made to detect the indications of AABW formation in this area.

It should be pointed out that the inverse model of Tziperman and Hecht (1988) does a poor job to resolve the vertical reference velocities. However, because of the significant convection in the Prydz Bay and its adjacent open ocean, things are somewhat different. Through a series of analyses and verifications of the obtained results, we conclude that here the vertical components can be partly resolved. The computed upwelling centers agree quite well with the areas of high krill biomass, suggesting the high correlation betwwen the upwelling phenomenon and krill concentration at Antarctic Divergence.

References

Dong Zhaoqian, Smith, N. R., Kerry, K. R. and Wright, S. (1984): Water masses and circulation in summer Prydz Bay. Essays on the Antarctic Scientific Expedition, China Ocean Press (in Chinese, with English abstract), Vol. 2, 1—24.

Gill, A. E. (1973): Circulation and bottom water production in the Weddel Sea. *Deep-Sea Res.*, 20, 111—140.

Gordon, A. L. (1983): Polar Oceanography. *Rev. Geophys. Space Phys.*, Vol. 21, No. 5, 1124—1131.

Grigor'yev, Y. A. (1967): Circulation of the surface waters in Prydz Bay. *Soviet Antarctic Expedition*, 7, 74—76.

Hogg, N. G. (1987): A least-square fit of the advective-diffusive equations to Levitus Atlas data. *J. Mar. Res.*, 45(9), 347—375.

Lawson, C. L. and Hanson, R. J. (1974): Solving Least Square Problems. Prentice—Hall, 340.

Marr, J. W. S. (1962): The natural history and geography of the Antarctic Krill (Euphausia Superba Dana). *Discovery Rep.*, 32, 33—464.

Mellor, M. (1960): Sea ice measurements at Mawson and Davis, 1954—1958. Australian National Antarctic Research Expeditions, Interim Report No. 19, Antarctic Division, Department of External Affairs, Melbourne, 33.

Needler, G. T. and Heath, R. A. (1975): Diffusion coefficients calculated from the Mediterranean salinity anomaly in the North Atlantic Ocean. *J. Phys. Oceanogr.*, 5, 173—182.

Shi Maochong, (1991): A study on the convection in Prydz Bay. Report of the 7th CHINARE, No. 3, Tsingtao University of Oceanography, Tsingtao. (in Chinese).

Smith, N. R., Dong Zhaoqian, Kerry, K. R. and Wright, S. (1984): Water masses and circulation in the region of Prydz Bay, Antarctica. *Deep-Sea Res.*, 31(9), 1121—1147.

Su Jilan and Pan Yuqiu (1987): On the shelf circulation north of Taiwan. *Acta Oceanol. Sinica*, 6 (supp. I), 1—20.

Tziperman, E. and Hecht, A. (1988): Circulation in the Eastern Levantine Basin determined by inverse methods. *J. Phys. Oceanogr.*, 18, 506—518.

Van der Sluis, A. (1969): Condition numbers and equlibration of matrices. *Numer. Math.*, 14, 14—23.

Wunsch, C. (1977): Determining the general circulation of the ocean: A preliminary Discussion. *Sci.*, 196, 871—875.

Yeskin, L. I. (1967): Is there an exchange of water between the Davis SEa and Prydz Bay? *Soviet Antarctic Expedition*, 7, 76—78.

Zverev, A. A. (1963): Currents in the Indian sector of the Antarctic. *Trudy Sovetskoi Antarkticheskoi Ekspeditsii*, 17, 144—155.